Modification of the Avrami Model for Application to the Kinetics of the Melt Crystallization of Lipids

Suresh S. Narine*, Kerry L. Humphrey, and Laziz Bouzidi

Alberta Lipid Utilization Program, Department of Agricultural, Food and Nutritional Science, University of Alberta, Edmonton, Alberta, Canada T6G 2P5

ABSTRACT: The Avrami model was developed to model the kinetics of crystallization and growth of a simple metal system. The original assumptions of the model do not apply for high-volume-fraction crystallizing lipids, although it is incorrectly and frequently applied. A modified form of the Avrami model, well-suited to complex lipid crystallization kinetics, is developed. It produces excellent fits to experimental data and allows the prediction of physically meaningful parameters, such as changes in nucleation rate and type, growth rate, morphology, and dimensionality. Morphological changes highlighted by time-resolved temperature-controlled polarized light microscopy support its application to crystallizing lipids. The kinetics of crystallization for six separate lipid samples were monitored by pulsed NMR, and fits were performed using the classical and modified Avrami model. In all cases, the modified model provided superior fits to the data compared with that of the classical model. The modified model supports the theory that lipids crystallize and grow into networks *via* very specific growth modes. Furthermore, the case is made that it is useful for interpreting crystallization kinetics of other systems such as polymer melts, which have nonconstant growth rates, dimensionalities, and nucleation conditions, and whose growth become diffusion-limited within specific regimes.

Paper no. J11426 in *JAOCS 83*, 913–921 (November 2006).

KEY WORDS: Avrami model, crystallization, kinetics, lipids.

The Avrami model is frequently used to evaluate the kinetics of crystallization and growth of lipids, and is purported to relate experimentally determined kinetics to growth modes and structure of the final lipid network. Unfortunately, the application of the Avrami equation in lipid crystallization literature is inconsistent. Three different fits of the Avrami model have produced significantly different values for the Avrami exponent and constant (see below). Some researchers suggest that only a portion of the crystallization curve should be fitted with the model, thereby ignoring important information about the entire crystallization process. It has also been suggested that there are a number of line segments within a typical data set that can each be fitted with the Avrami model, and researchers have arbitrarily chosen one segment to fit with the model, without any justification. In fact, the crystallization kinetics of most lipid systems are not characterized by conditions that the Avrami model assumes are valid.

*To whom correspondence should be addressed at 4-10 Agricultural/Forestry Centre, University of Alberta, Edmonton, Alberta, Canada T6G 2P5. E-mail: suresh.narine@ualberta.ca

This communication reviews the development of the Avrami model and examines crystallization data from a number of lipid systems. A modification to the Avrami model is proposed that does not violate the assumptions of the original model and provides excellent fits of crystallization data from lipids.

Assumptions of the Avrami model. The Avrami equation is used extensively to model the crystallization behavior of metallic melts, polymers, and more recently, lipids, and is related to the problem of impinging waves, a problem first solved by Poisson (1). It is important to note that essentially identical treatments to that of Avrami were proposed by Kolmogorov (2), Johnson and Mehl (3), and Evans (4), and in many instances, the model is referred to as the Johnson–Mehl–Avrami–Kolmogorov model (JMAK). Developments for various types of geometry have been reported by various authors, and more importantly, adhere to the same assumptions (5).

The basic isothermal expression of the Avrami equation is given by:

$$\theta(t) = \frac{F(t)}{F_\infty} = 1 - e^{-At^m} \qquad [1]$$

where $\theta(t)$ is the relative crystallinity at time t, $F(t)$ is the absolute crystallinity at time t, F_∞ is the final absolute crystallinity, A is the crystallization rate constant containing the nucleation and growth rates, and m is the Avrami index or exponent.

The model assumes a constant linear crystal growth rate, G, and that nucleation is either instantaneous (athermal) or sporadic (thermal). In either case, the m term will be different for spherulitic growth, continuous nucleation, growth in less than three dimensions, and heterogeneous nucleation on planar or linear defects (6). For a good summary of the nature of nucleation, growth, and dimensionality in terms of the values of A and m, the reader is referred to Sharples (5).

In practice, Equation 1 is fitted to experimental data such as DSC measurements, dilatometry measurements, and pulsed NMR (p-NMR) measurements, which all have been used to determine the degree of crystallization of a lipid sample as a function of time. The fits produce an experimentally determined value for the Avrami exponent, which then should provide an indication of the nucleation type, growth order (dimensionality), and geometry of the growing entities. Of course, the Avrami constant can also be extracted from the fit, but extracting predictive information from this value requires additional

Copyright © 2006 by AOCS Press

information on one or more of the crystal growth rate, *G*, or the number of germ nuclei per unit volume *N*, parameters. Nevertheless, the comparative values of the Avrami constant for changes in chemical nature and/or environmental conditions are useful indicators of physical changes in the growth rate and nucleation rate.

To describe nonisothermal crystallization quantitatively, a number of models have been proposed. The majority of them are based on the Avrami equation, but the isothermal model is extended by using some integral form to take into account the evolution of temperature with time. In a commonly used model that is based on Avrami model, Equation 1 is simply used along with a growth rate constant corrected for the effect of cooling rate. Notice that the physical meaning of the growth rate constant and the Avrami exponent cannot be related in a simple way to the nonisothermal case (7). For reviews on the development of the Avrami equation, the original Avrami papers as well as that of a number of other authors are recommended (8–12).

Problems associated with fitting the Avrami model to experimental data. The Avrami model is difficult to apply to the entire range of the crystallization event, mainly because the rate of crystallization (growth rate) and the dimensionality of growth in the model are assumed to be linear and constant, where this is clearly not the case for crystallizing lipids, and because the type of nucleation as a function of time does not change. Furthermore, even for well-behaved systems, a secondary crystallization process often occurs after spherulitic growth (as in Fig. 1), as a result of melt present in the interstitial spaces. Further complications arise owing to situations when the nucleation mode is a mixture of thermal and athermal nucleation, resulting in fractional exponents. Simulations for the Avrami equation (Eq. 1), for various integer values of *m* and a range of values of *A* (within the range of experimentally determined values of *A* and *m* in the lipid literature), clearly demonstrate that any minor deviation from a perfect sigmoid in the experimentally determined data essentially results in a superposition of different Avrami constants and exponents within the same fit (13–15). In practice, many approaches in the literature attempt to explain (usually without experimental evidence) lower-than-expected or noninteger Avrami exponents derived from experimentally obtained data.

Crystallizing lipids and nonadherence to Avrami kinetics. In the crystallization of TAG lipids, a number of common phenomena can contribute to increases or decreases of the rate of increase of SFC as a function of time. These include the following: (i) Secondary nucleation often occurs once a lipid sample has begun crystallizing, leading to a change in the type of nucleation (different from original germ nuclei) as a result of reduced surface free energy on the surface of crystallized material. (ii) Many natural lipids are composed of a variety of molecular "families" having similar requirements for the activation free energy of molecular diffusion and for the activation free energy for formation of stable nuclei. As the conditions for different "families" are met over the entire crystallization event, changes occur in the growth rate and growth dimension. (iii) Crystallizing lipids are extremely prone to metastable phases, and polymorphic transformations often occur in the midst of crystallization of the same or different "families" of TAG molecules. This definitely leads to a change in dimensionality and may lead to changes in growth rate as well. (iv) The process of crystallization increases the barrier to molecular transport as a result of increased viscosity (owing to both changes in temperature as the sample is cooled and changes in the volume of crystallized material), leading to decreased growth rates. (v) Evolution of heat as the sample crystallizes can result in re-melt or in localized regions of high and low viscosity owing to heat transfer. This results in an unequal nonisotropic growth rate. (vi) Considering only nuclei present in the melt at the inception of the crystallization process for a certain fraction of the TAG may not be applicable. The model needs to consider entirely new germ nuclei for a later-crystallizing fraction or family of TAG molecules.

As a result of the large number of events that can occur that change the rate of increase of SFC over time, the observation of a perfect sigmoidal relationship is rare.

In trying to fit the Avrami model to data of crystallizing lipids, some authors (16,17) have suggested eliminating different arbitrary regions of the solid fat content (SFC)–time curve from the fit, hypothesizing that there is an appropriate region of constant radial growth rate with no crystal impingement. There is no supporting evidence for this growth mode within these limits in the lipid literature, nor are there theoretical reasons why the growth mode of the fat should be a constant radial growth. Setting arbitrary boundaries for the fitting of the data to the Avrami model clearly will lead to important kinetic effects being ignored; and because different authors choose different boundaries, the reports of Avrami constants and exponents in the lipid literature must be viewed with caution.

The actual fitting of the Avrami model to experimental data has been accomplished *via* a series of modifications of the form

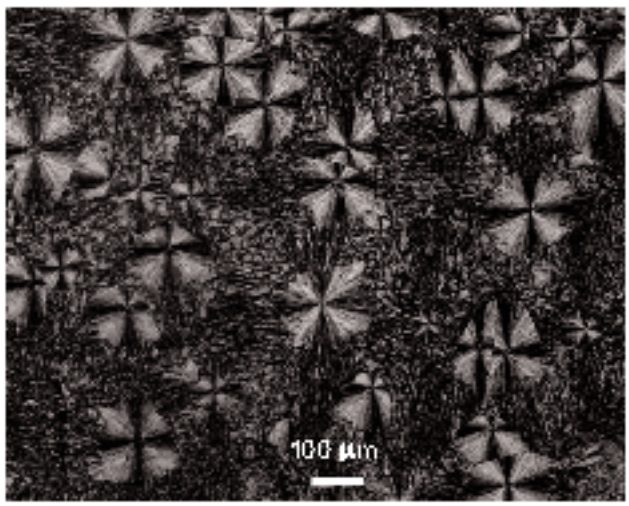

FIG. 1. High-resolution polarized light micrograph of the 1,3-dilauroyl-2-stearoyl-*sn*-glycerol (LaStLa) system showing a secondary crystallization process occurring after spherulitic growth, from melt present in the interstitial spaces.

of Equation 1. There is a nonlinear fit (18,19), a partially linearized fit (20–22), a linear fit (16,23), and the modified Avrami–Erofeev fit, also known as the modified form of the Avrami equation (24,25) which has been convincingly shown to be incorrect (26). Foubert *et al.* (27) highlighted the major issues associated with the linearized versions of the Avrami equation such as the transformation of the measurement errors, the clustering of data points at high values of ln(*t*), and the difficulties in obtaining confidence ranges for the estimated parameters.

EXPERIMENTAL PROCEDURES

When referring to sample holding temperature as well as cooling and heating rates, all temperatures are reported to a certainty of ±0.5°C unless otherwise noted.

Sample preparation. Binary mixtures of 1,2-dilauroyl-stearoyl-*sn*-glycerol (LaLaSt) and 1,3-dilauroyl-2-stearoyl-*sn*-glycerol (LaStLa) (97% or greater purity) were prepared in concentrations of 0, 20, 90, and 100% (w/w) by first heating the pure TAG to 90°C and stirring vigorously for 5 min with a mechanical stirrer to ensure homogeneity before sampling. A blend of 10% fully hydrogenated canola in soybean oil (referred to as the 10% Canola sample) was prepared in a similar manner. The commercial vegetable shortening Crisco was simply stored for sampling. The prepared samples were stored in glass jars at –10°C to minimize oxidation.

NMR. The instrument used in the investigations was the minispec mq SFC analyzer (Bruker, Milton, Ontario, Canada), which is a pulse magnetic resonance spectrometer with a temperature-controlled measurement chamber. The data sampling procedure was fully automated, and the SFC was calculated and displayed by computer software. Each of the fat mixtures was held for 5 min at 90°C before being vigorously stirred for 2 min using a motorized mechanical stirrer. The fat was quickly pipetted into the bottom 3.5 ± 0.1 cm portion of the NMR tubes. Sample tubes were stored at –10°C.

Samples were heated to 90°C and held for 5 min, then cooled in a programmable water bath to 67°C. The samples were then inserted in the temperature-controlled p-NMR spectrometer and cooled to a final temperature of 15°C. The measurement continued for 60 min after reaching the final temperature. All samples were run in duplicate with a constant cooling rate of 3°C/min.

Microscopy. A high-resolution polarized light microscope, equipped with a high-resolution Hamamatsu Digital Camera and a Linkam LTS 350 temperature-controlled stage, was used. The microscope/camera assembly was controlled by Openlab 3.0.8 software (Improvision. Warwick, United Kingdom). The fat mixtures were held at 90°C for 5 min before being vigorously stirred for 2 min using a motorized mechanical stirrer. A small drop of fat was placed in the center of a microscope slide and covered loosely with a cover slip. The slide was then placed on a hot plate at 90°C to melt the fat, the cover slip was pressed down into the drop of liquid fat, and the excess fat was removed with a paper towel.

The prepared slides were processed in the Linkam stage by holding the slide at a temperature of 90°C for 5 min and then cooled at a rate of 3°C/min to the final temperature of 15°C. The images were captured during the cooling process at intervals of 30 s, with melting and recrystallization occurring after each image was captured. The samples were then held at the final temperature for 60 min, with pictures being captured at the end of the holding period.

RESULTS AND DISCUSSION

Traditional fits applied to experimental data. The curves shown in Figures 2–5 were plotted using GraphPad 4 Prism software version 4.02 (www.graphpad.com), and the plotted data were fitted using the fit methods provided with the software.

Unlike the SFC–time curves generated by simulating the Avrami equation, the experimentally determined SFC vs. time curves for lipid samples do not demonstrate the monotonic increase demonstrated by the Avrami sigmoids as shown in Figure 2. These curves represent experimentally determined values for real lipid samples. Clearly there are significant kinetic events still occurring outside the 0–10% and 90–100% fractional SFC boundary. (The dotted horizontal lines in Figure 2 indicate the boundaries of 10 and 90% crystallization.) The most evident disruptions in the SFC–time curves are demonstrated in Figure 2c at 2000 and 2100 s and in Figure 2f at 1400 s. Such changes in growth kinetics could suggest a change in the molecular nature of the TAG participating in the crystallization, in the thermodynamic driving forces propelling crystallization, in the growth mode of the crystals, or limitations to molecular transport due to increases in viscosity and steric hindrances. Rate changes from rapid increases in percent SFC to a slower rate of increase in percent SFC indicate a region of more laborious growth, potentially owing to the crystallization of a halting agent or to a fraction requiring more organization time to crystallize, or to the presence of a molecular species that is not easily incorporated into the crystal lattice due to shape considerations, or to a requirement for more aggressive conditions of undercooling than provided by our 3°C/min rate.

The partially linearized fit and the nonlinear fit of Equation 2 have been applied to the data set shown in Figure 2. The partially linearized fits of the Avrami model have been performed using the following form of Equation 1:

$$-\ln[1-\theta] = At^m \qquad [2]$$

The curves of $-\ln(1-\theta)$ vs. time have r^2 values ranging from 0.9029 (100% LaStLa) to 0.5328 (10% Canola). The fit is notably poor for all data sets when the data are graphed as percent SFC vs. time as shown in Figure 3 for the 20% LaLaSt sample. The simulated data are then reverse-engineered into percent SFC and time and plotted in the same chart as the original data. The fit is relatively good only for higher portions of the SFC vs. time curve, while the shape of the lower portion and the variations in slope within each curve are ignored. This suggests that the growth structures established in the initial stages of the crystal-

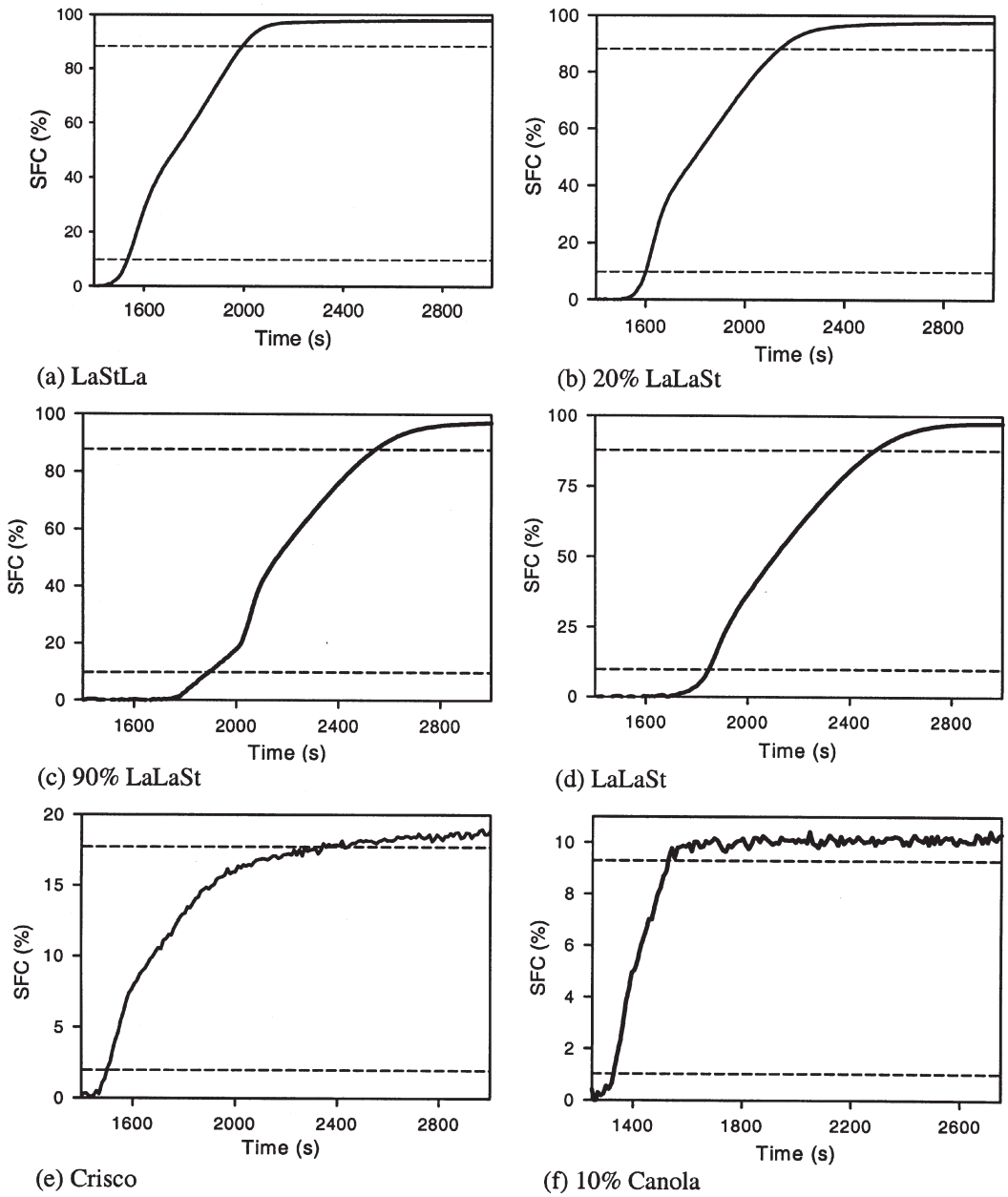

FIG. 2. Experimentally determined solid fat content (SFC) vs. time curves for lipid samples. LaLaSt, 1,2-dilauroyl-stearoyl-*sn*-glycerol; for other abbreviation see Figure 1.

lization process, as well as variations in the rate of increasing percent SFC, are not being addressed. This exclusion is particularly alarming as some authors extend their discussions of the fit exponents and constants procured by this method to the morphological characteristics shown by the lipid system (14,28). Of importance, this particular Avrami fit does not take into consideration the minor variations within the growth curve, which can result in significant changes in A and m.

The nonlinear fits have been performed using the original form of the Avrami equation shown in Equation 1 where Y = SFC (%) and X = time. The r^2 values for the fits range from 0.9833 (for the 10% fully hydrogenated canola in soybean oil) to 0.9981 (for the 100% LaLaSt sample). Compared with the fits achieved with the partially linearized fit method, the nonlinear fits are better as the r^2 values are higher, and both the upper and lower portions of the curve fit reasonably well. There are no obvious deviations in the fit for the Crisco and 10% Canola samples, which indicates that this fit method works well for the commercial shortening sample due to the molecular complementarities of the shortening system. This is to be expected as commercial shortenings are engineered not to demonstrate eutectic behaviors or changes in the monotonic growth of the structures in the lipid system. However, for all other samples where obvious changes in the rate of increasing percent

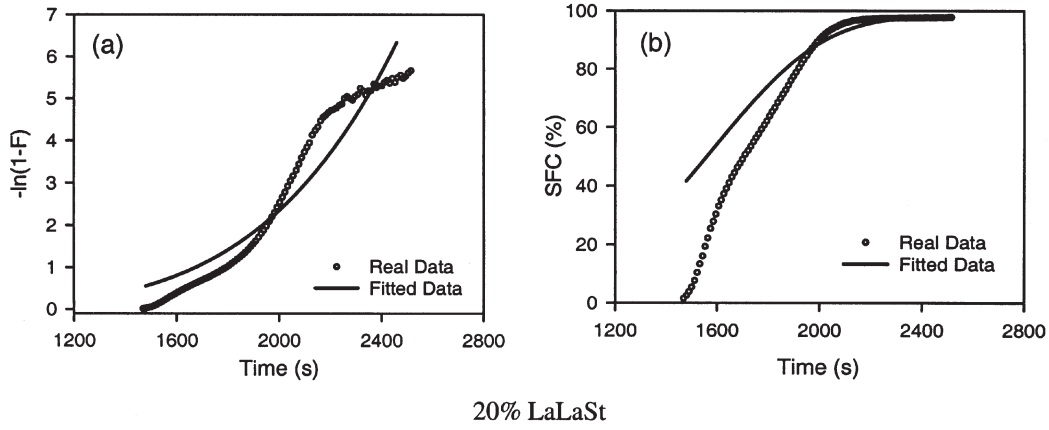

FIG. 3. (a) Partially linearized fits of the Avrami model and (b) reverse-engineered fit into percent SFC and time and plotted with the original data of the 20% LaLaSt sample. *F* is the absolute crystallinity at time *t*; for other abbreviations see Figures 1 and 2.

SFC are present, the model does not fit the data well. The deviations from the original data of the fitted line are highlighted by the arrows on Figure 4a and 4b showing the results of the data fit with this method for the 100% LaStLa and 90% LaLaSt samples, respectively.

Although the partially linearized fit method works well for sigmoidal, monotonic, first-order processes, it does not and should not work for processes demonstrating kinetic changes, as separate, distinct growth modes are encountered during the network formation. Clearly, using the approaches just presented to fit our experimental data is inadequate.

Modification of the Avrami model. From the foregoing discussion, it is clear that most lipid crystal networks demonstrate nonsigmoidal SFC vs. time curves. The potential reasons for changes in the rate of increase of SFC have been discussed earlier. Furthermore, most lipid crystal network systems to which the Avrami model has been fitted in the literature, and in particular the systems considered in this work, demonstrate a high volume fraction of crystalline material. However, the Avrami model is highly dependent on the approximation using low values of crystallization. Therefore, in addition to the fact that a constant growth rate, dimensionality, and nucleation conditions are not normally applicable in most lipid systems, the approximation is not applicable, since it is only valid at conditions of relatively low crystallinity.

We propose here a modification to the Avrami model that allows us to apply Avrami-type kinetics to the entire range of growth of the lipid network and that allows for the non-Avrami-type kinetics demonstrated by crystallizing lipid systems. We submit that the Avrami model as explained earlier is only valid for a crystallizing lipid network from $t = 0$, when the radial growth rate G is constant and the nucleation conditions do not change. As soon as these conditions are no longer applicable, we propose that the system be regarded as the end of one crystallization event, and the beginning of a second event, and so forth until the network is fully formed. The crystallization of a lipid network system could therefore be thought of as a succession of p different crystallization events occurring in steps. Fur-

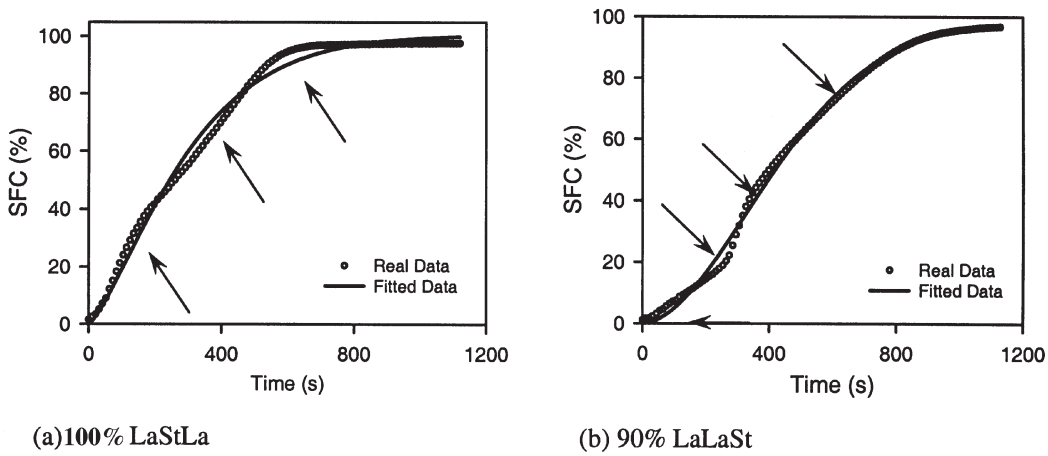

FIG. 4. Results of the nonlinear fit method using the original form of the Avrami equation given by Equation 1. (a) 100% LaStLa; (b) 90% LaLaSt. For abbreviations see Figures 1 and 2.

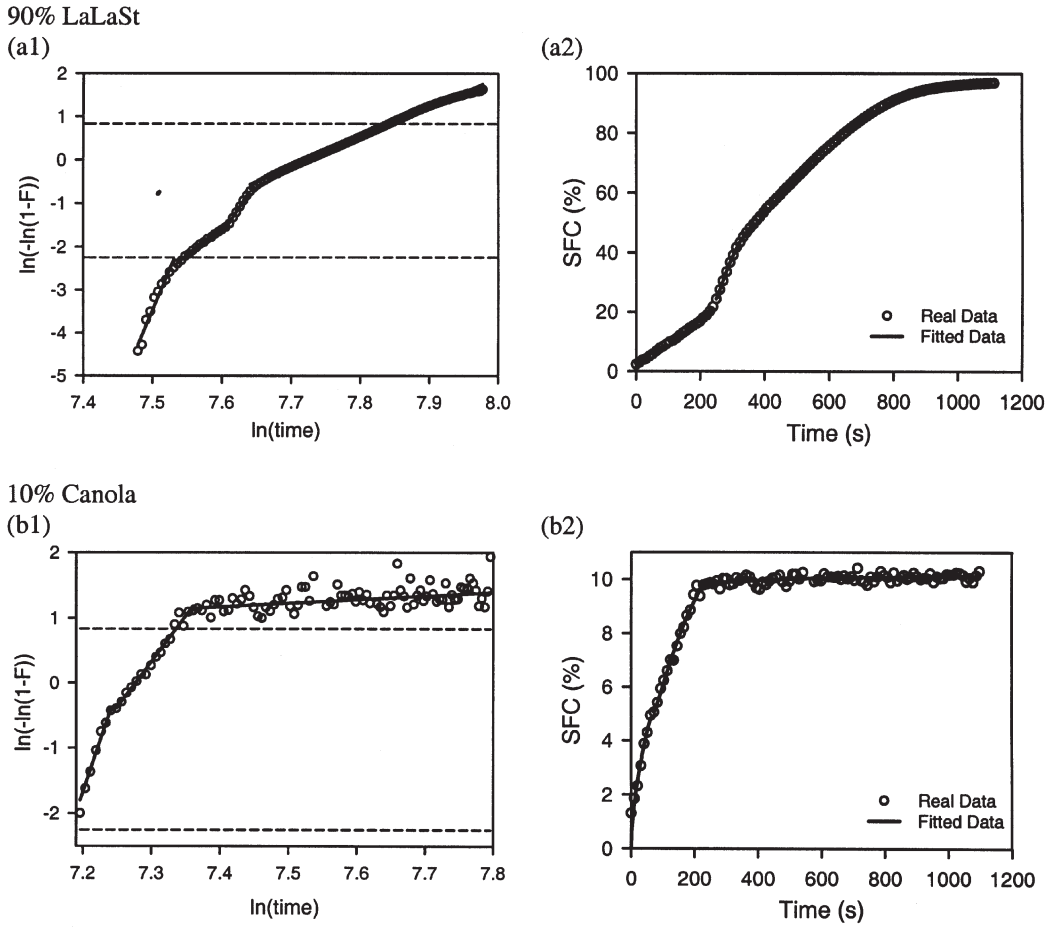

FIG. 5. Ln[–ln(1 – *F*)] vs. ln(*t*) plots from experimentally-determined SFC–time data. (a1) 90% LaLaSt and (b1) 10% Canola and nonlinear fits of experimental data with identified line segments using Equation 8 to fit the data. (a2) 90% LaLaSt and (b2) 10% Canola. For abbreviations see Figures 1 and 2.

thermore, each step *i* is characterized by a constant growth rate G_i and constant nucleation conditions and occurs for a limited, relatively small degree of crystalline growth. Such conditions allow the assumptions under which the Avrami equation was developed, as discussed earlier, to be valid. The crystallized material preceding each new crystallization event is essentially viewed as a part of the environment within which a "new" sample is being crystallized. Each step (or single crystallization) would begin after an incubation time τ_i. The first step, which starts at $t = 0$ (the first event begins without incubation, i.e., $\tau_1 = 0$), can be described by an Avrami equation:

$$\frac{F_1(t)}{F_{1\infty}} = 1 - \exp[-A_1 t^{m_1}] \quad [3]$$

where $F_1(t)$ is the absolute crystallinity at time t, $F_{1\infty}$ is the crystallinity at some time when either the growth rate or the nucleation conditions change, and A_1 and m_1 are the Avrami constant and exponent applicable to the nucleation, growth, and dimensionality of the crystallizing lipid over that segment of time where such conditions are constant. The second segment will take place after an incubation time τ_2 and can be described by

$$\frac{F_2(t)}{F_{2\infty}} = 1 - \exp[-A_2(t-\tau_2)^{m_2}], \text{for } t > \tau_2 \quad [4]$$

and so forth. In this manner, the Avrami equation for step *i* is given by

$$\frac{F_i(t)}{F_{i\infty}} = 1 - \exp[-A_i(t-\tau_i)^{m_i}], \text{for } t > \tau_i \quad [5]$$

At each step, the crystallization is characterized by $F_i(t)$, a single absolute crystallinity at time t, $F_{i\infty}$, the ultimate absolute crystallinity for the appropriate segment, and A_i and m_i, its Avrami parameters ($i = 1, \ldots, p$).

By using the commonly known Heaviside function,

$$H(t-c) = u_c(t) = \begin{cases} 0 & \text{if } t<c \\ 1 & \text{if } t \geq c \end{cases}, \quad [6]$$

Equation 5 may be written as

$$F_i(t) = F_{i\infty}\{-\exp[-A_i(t-\tau_i)^{m_i}]\} \cdot H(t-\tau_i) \quad [7]$$

The total absolute crystallinity will be the sum of the p individual absolute crystallinities:

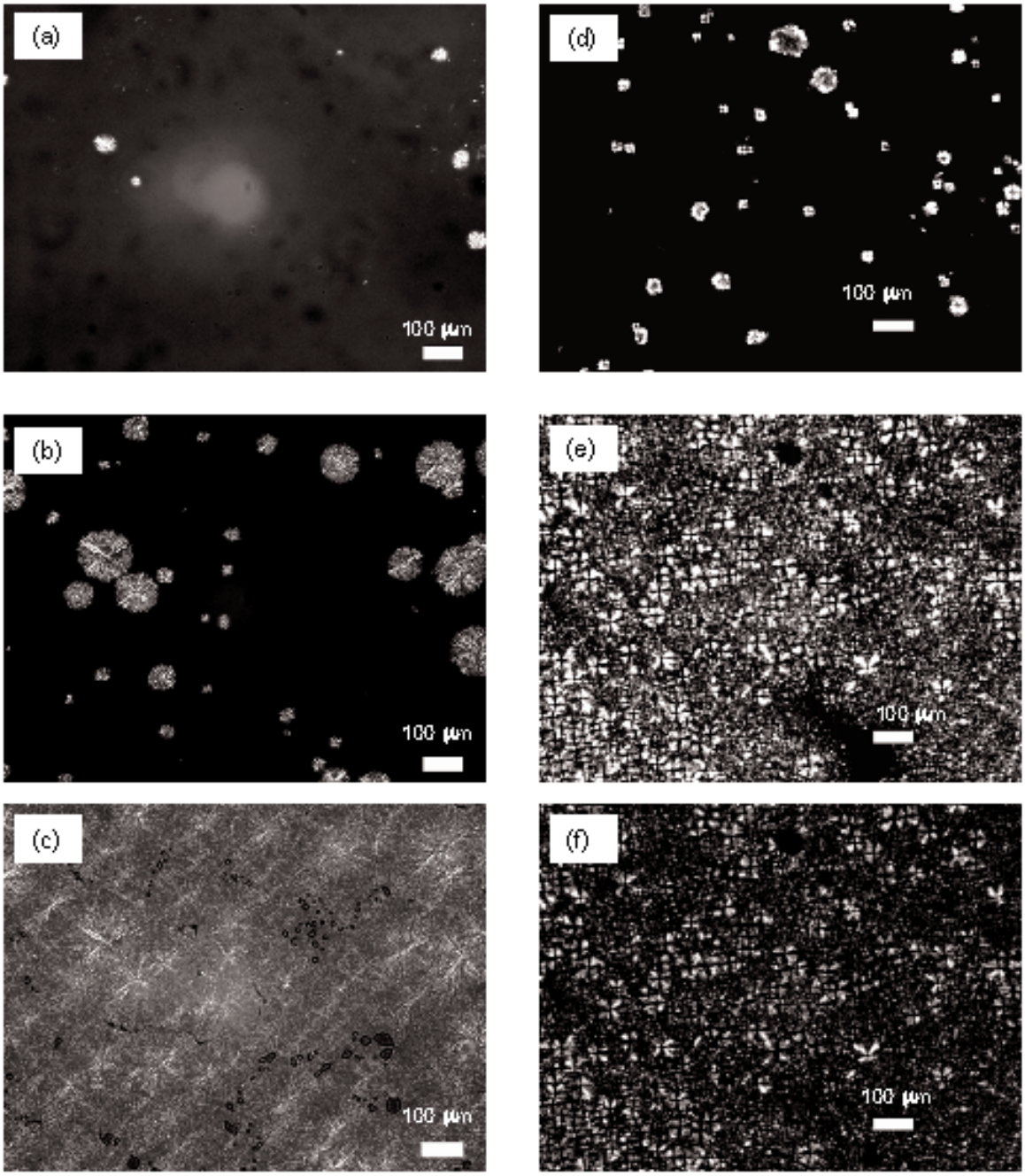

FIG. 6. High-resolution polarized light micrographs of the LaStLa and LaLaSt systems cooled from 90°C at a rate of 3°C/min showing three successive distinct regimes of growth. Micrographs were taken for LaStLa at (a) 1740 s, (b) 1770 s, (c) 1950 s, and for LaLaSt at (d) 1900 s, (e) 1930 s, (f) 1990 s. For abbreviations see Figures 1 and 2.

$$F(t) = \sum_{i=1}^{p} F_i(t) = \sum_{i=1}^{p} F_{i\infty}\{1 - \exp[-A_i(t-\tau_i)^{m_i}]\} \cdot H(t-\tau_i) \qquad [8]$$

We can think of the Heaviside function as a switch that is off until $t = \tau_I$, at which point it turns on and introduces crystallization i into play.

Application of the modified model to lipid systems. It is clear from Equation 8 that this modified model must be used in a semiempirical manner. For example, the value of p and the individual values of τ_2 to τ_p must be determined empirically.

The need to define unambiguous time domains for each crystallization segment was accomplished by plotting ln[–ln(1 – F)] vs. ln(t) from experimentally determined SFC vs. time data. To determine the end points of the line segments in the linearized data unambiguously, the following protocol was followed. To begin, a line was fitted to the first four data points in the sequence. If the r^2 value for the line was less than 0.95, the

points were discarded. If the r^2 value for the line was greater than or equal to 0.95, the next two data points in the sequence were added to the line and a new r^2 value was computed. As long as the r^2 value did not fall below 0.95, the line continued to lengthen, two data points at a time. When the r^2 value for the line fell below 0.95, the last two data points added to the line were removed (so that the resulting line had an r^2 value within the acceptable range), and the line segment was determined to be terminated. The next four data points in the large array were then chosen to be the first four points in the new line and the algorithm for determining the end points of the line continued. In this way, the researcher need not impart his or her discretion in discerning the end points of each line segment. The source code for this algorithm was compiled in Borland Turbo C++ version 5.02. Note that the limiting r^2 value can be changed easily using the program. This process therefore easily defines the boundaries of each segment of crystallization to be treated individually.

For all data sets, the algorithm clearly produces a sequence of straight lines for each set, which emphasizes the change in increasing percent SFC. Multiple straight lines are even apparent in the samples for which good fits were achieved with the nonlinear method, suggesting that important changes in the SFC growth rate can be hidden when fitted with this method. There are four obvious straight line segments for the 90% LaLaSt, whereas the remaining data sets have three obvious line segments each. Once the boundaries of the different line segments are identified, this provides the values of τ_2 to τ_p and p required to use Equation 8 to fit the data. The result is a series of sigmoids, which provides exceptional fits to the experimental data. The straight line and sigmoid fits are illustrated in Figure 5a and 5b for the 90% LaLaSt and the 10% Canola samples, respectively.

Except for the rightmost lines in the 100% LaLaSt, Crisco, and 10% fully hydrogenated canola in soybean samples (figure not shown), the straight line fits and the sigmoid fits have r^2 values greater than 0.95. For the few that are lower, these can be explained by the fact that those segments had a small number of data points in the region to be fitted (meaning that even one small deviation from an original data point may lower the r^2 value significantly), or that variations in the original data due to the noise of the instrument will heighten the number of actual data points not lying on the line of best fit. However, all the fits using our modified Avrami model are notably better than any of the other methods used to fit the data. Furthermore, the fit parameters now have physical meaning, whereas before the reported values were not representative of the model's underlying assumptions.

Clearly, these plots can be fitted to a multiplet of straight lines; each line segment represents a sigmoid when converted back to SFC vs. time plots and defines the crystallization pertaining to different Avrami-type kinetics. Furthermore, these plots account for the variation in kinetics because separate Avrami constants and exponents can be extracted for each separate segment. This is of course appropriate, since each segment in the first place demonstrated different kinetics because the growth mode (growth rate, dimensionality of growth, nucleation type) of the crystallizing lipid is different within each segment.

Supporting microstructural evidence. There is little variation in the determined values of the Avrami exponent, which seemed to fluctuate around a value of 1, but there are significant changes in the Avrami constant. It is difficult to relate quantitatively morphological changes in microscope images of the samples with the time segments for particular fits, since the heat and mass transfer and dimensionality limitations on a microscope slide are quite different for samples crystallizing in a p-NMR sample tube (even though the cooling rates are comparable). However, one can point to qualitative changes of morphology to support the claim of separate growth modes in the different samples. Examples are shown in Figure 6. The LaStLa and LaLaSt samples clearly demonstrate three separate growth modes, characterized by very different Avrami constants, and similar Avrami indices. As is demonstrated in Figure 6, both lipid systems also demonstrate three very different morphologies at different points in their crystallization process.

ACKNOWLEDGMENTS

The authors acknowledge the technical contributions of Dr. Tomas Kutek, Marc Boodhoo, and Ereddad Kharraz. The financial support of the National Sciences and Engineering Research Council, Bunge Oils, AVAC Ltd., and Archer Daniels Midland is gratefully acknowledged.

REFERENCES

1. Poisson, S.D., *Recherches sur la probabilité des jugements en matière criminelle et en matière civile*, Bachelier, Paris, 1837.
2. Kolmogoroff, A.N., On the Statistical Theory of Metal Crystallization, *Izv. Akad. Nauk SSSR, Ser. Math. 1*:335–360 (1937).
3. Johnson, W.A., and R.F. Mehl, Reaction Kinetics in Processes of Nucleation and Growth, *Trans. Am. Inst. Min. Metall. Eng. 135*:416–442 (1939).
4. Evans, U.R., Laws of Expanding Circles and Spheres in Relation to the Lateral Growth of Surface Films and the Grain Size of Metals, *Trans. Faraday Soc. 41*:365–374 (1945).
5. Sharples, A., Overall Kinetics of Crystallization, in *Introduction to Polymer Crystallization*, edited by A. Sharples, Edward Arnold Ltd., London, 1966, pp. 44-59.
6. Christian, J.W., *The Theory of Transformations in Metals and Alloys*, Pergamon Press, London, 1975.
7. Achilias, D.S., G.Z. Papageorgiou, and G.P. Karayannidis, Isothermal and Nonisothermal Crystallization Kinetics of Poly(propylene terephthalate), *J. Polym. Sci. B-Polym. Phys. 42* 3775–3796 (2004).
8. Avrami, M., Kinetics of Phase Change. I. General Theory, *J. Chem. Phys. 7*:1103–1112 (1939).
9. Avrami, M., Kinetics of Phase Change. II. Transformation-Time Relations for Random Distribution of Nuclei, *Ibid. 8*:212–224 (1940).
10. Avrami, M., Granulation, Phase Change and Microstructure. Kinetics of Phase Change. III, *Ibid. 9*:177–184 (1941).
11. Woldt, E., The Relationship Between Isothermal and Nonisothermal Description of Johnson–Mehl–Avrami–Kolmogorov Kinetics, *J. Phys. Chem. Solids 53*:521–527 (1992).
12. Cheng, S.S.D., and B. Wunderlich, Modification of the Avrami

Treatment of Crystallization to Account for Nucleus and Interface, *Macromolecules 21*:3327–3328 (1988).
13. Khanna, Y., and T. Taylor, Comments and Recommendations on the Use of the Avrami Equation for Physico-chemical Kinetics, *Polym. Eng. Sci. 28*:1042–1045 (1988).
14. Metin, S., and R. Hartel, Thermal Analysis of Isothermal Crystallization Kinetics in Blends of Cocoa Butter with Milk Fat or Milk Fat Fractions, *J. Am. Oil Chem. Soc. 75*:1617–1624 (1998).
15. Toro-Vazquez, J., E. Dibildox-Alvarado, M. Charo-Alonso, V. Herrera-Coronado, and C. Gomez-Aldapa, The Avrami Index and the Fractal Dimension in Vegetable Oil Crystallization, *Ibid. 79*:855–866 (2002).
16. Toro-Vazquez, J., E. Dibildox-Alvarado, V. Herrera-Coronado, and M. Charo-Alonso, Triacylglyceride Crystallization in Vegetable Oils: Application of Models, Their Measurements, and Limitations, in *Crystallization and Solidification Properties of Lipids*, edited by N. Widlak, R. Hartel, and S. Narine, AOCS Press, Champaign, Illinois, 2001, pp. 53–78.
17. Herrera, M., C. Falabella, M. Melgarejo, and M. Añon, Isothermal Crystallization of Hydrogenated Sunflower Oil: II. Growth and Solid Fat Content, *J. Am. Oil Chem. Soc. 76*:1–6 (1999).
18. Dibildox-Alvarado, E., and J. Toro-Vazquez, Isothermal Crystallization of Tripalmitin in Sesame Oil, *Ibid. 74*:69–76 (1997).
19. Narine, S.S., and A.G. Marangoni, Microstructure, in *Fat Crystal Networks*, editd by A.G. Marangoni, Marcel Dekker, New York, 2004, pp. 179–255.
20. Vanhoutte, B., I. Foubert, F. Duplacie, A. Huyghebaert, and K. Dewettinck, Effect of Phospholipids on Isothermal Crystallization and Fractionation of Milk Fat, *Eur. J. Lipid Sci. Technol. 104*:738–744 (2002).
21. Campos, R., S. Narine, and A.G. Marangoni, Effect of Cooling Rate on the Structure and Mechanical Properties of Milk Fat and Lard, *Food Res. Int. 35*:971–981 (2002).
22. Graydon, J., S. Thorpe, and D. Kirk, Determination of the Avrami Exponent for Solid State Transformations from Non-Isothermal Differential Scanning Calorimetry, *J. Non-Cryst. Solids 175*:31–43 (1994).
23. Chong, C., Crystallization of Palm Oil Product*s,* in *Crystallization and Solidification Properties of Lipids*, edited by N. Widlak, R. Hartel, and S. Narine, AOCS Press, Champaign, Illinois, 2001, pp. 110–119.
24. Ng, W., and C. Oh, A Kinetic Study on Isothermal Crystallization of Palm Oil by Solid Fat Content Measurements, *J. Am. Oil Chem. Soc. 71*:1135–1139 (1994).
25. Herrera, M., M. de Leon Gatti, and R. Hartel, A Kinetic Analysis of Crystallization of a Milk Fat Model System, *Food Res. Int. 32*:289–298 (1999).
26. Marangoni, A.G., On the Use and Misuse of the Avrami Equation in Characterization of the Kinetics of Fat Crystallization, *J. Am. Oil Chem. Soc. 75*:1465–1467 (1998).
27. Foubert, I., K. Dewettinck, and P.A. Vanrolleghem, Modelling of the Crystallization Kinetics of Fats, *Trends Food Sci. Technol. 14*:79–92 (2003).
28. Martini, S., M. Herrera, and R. Hartel, Effect of Cooling Rate on Crystallization Behavior of Milk Fat Fraction/Sunflower Oil Blends, *J. Am. Oil Chem. Soc. 79*:1055–1062 (2002).

[Received June 19, 2006; accepted August 8, 2006]